

Synthesis and Characterization of the Electron-Rich Iron Hydride $\text{HFe}(\text{CO})_2(\text{P}(\text{OPh})_3)_2^-$ and Its Ligand-Based Redox Substitution with Thiolates

Marcetta Y. Darensbourg,* Sheryl A. Wander, and Joseph H. Relbendspies

Department of Chemistry, Texas A&M University, College Station, Texas 77843

Received March 16, 1992

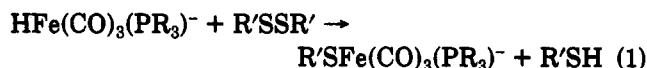
The bis(phosphite) anionic hydride $[\text{Et}_4\text{N}^+][\text{HFe}(\text{CO})_2(\text{P}(\text{OPh})_3)_2^-]$ has been synthesized by deprotonation of $\text{H}_2\text{Fe}(\text{CO})_2(\text{P}(\text{OPh})_3)_2$ with $[\text{Et}_4\text{N}^+][\text{OH}^-]$. The $[\text{Et}_4\text{N}^+][\text{HFe}(\text{CO})_2(\text{P}(\text{OPh})_3)_2^-]$ salt was characterized by X-ray diffraction, crystallizing in the monoclinic space group Cc (No. 9) with $a = 15.821$ (4) Å, $b = 15.168$ (3) Å, $c = 19.125$ (5) Å, $\beta = 111.05$ (2)°, $V = 4283$ (2) Å³, and $Z = 4$. In the solid state the hydride anion has a distorted-trigonal-bipyramidal geometry in which the hydride ligand occupies an axial position with an Fe-H bond distance of 1.47 Å. One triphenyl phosphite ligand is cis to the hydride and has an Fe-P_{eq} bond distance of 2.076 (1) Å, the other is trans with Fe-P_{ax} = 2.083 (1) Å, and $\angle \text{P}_{eq}\text{-Fe-P}_{ax}$ is 103.2 (1)°. Analysis of the $\nu(\text{CO})$ infrared and ¹H NMR results imply that in solution the isomer in which both phosphite ligands are cis to the hydride predominates as the ground-state structure. The alkali-metal cations Na⁺ and K⁺ form contact ion pairs with $[\text{HFe}(\text{CO})_2(\text{P}(\text{OPh})_3)_2^-]$, specifically interacting with the carbonyl oxygens of both CO ligands simultaneously. The $[\text{HFe}(\text{CO})_2(\text{P}(\text{OPh})_3)_2^-]$ anion reacts with PhSSPh to yield $[\text{Et}_4\text{N}^+][(\text{PhS})\text{Fe}(\text{CO})_2(\text{P}(\text{OPh})_3)_2^-]$ but is unreactive with MeSSMe and *t*-BuSS-*t*-Bu.

Anionic transition-metal hydrides typically require the presence of carbonyl ligands to stabilize the electron-rich metal centers.^{1,2} The substitution of one CO by a phosphorus-donor ligand has been shown to lend greater nucleophilic (hydride anion transfer) character to such hydrides as *cis*-HM(CO)₄PR₃⁻ (M = Cr, W) vs HM(CO)₅,³ even though the homolytic bond strength of M-H is enhanced by phosphine substitution.⁴

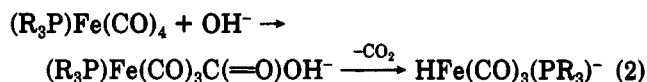
Monomeric iron hydrides $\text{HFe}(\text{CO})_4^-$ and $\text{HFe}(\text{CO})_3(\text{PR}_3)^-$ have also been compared for structural and reactivity differences.⁵ The latter are particularly interesting in that the PR₃ ligand (R = Ph, Me, Et) is in the trans position, as expected for a trigonal-bipyramidal structure. However, for R = OPh, the ligand is cis to the axial Fe-H.⁶ Most peculiar was the small (maximum of 12 Hz) and variable P-H coupling constant of the trans derivatives.⁵ The temperature dependence was ascribed to slight structural changes induced by solvation or solvent dielectric constant differences upon varying the temperature or nature of the solvent.⁷ In contrast, *cis*-HFe(CO)₃P(OPh)₃⁻ displayed a moderate J_{PH} value of 52 Hz.⁸ Regardless of isomeric form, the substituted iron hydrides were considerably more reactive than $\text{HFe}(\text{CO})_4^-$ toward electrophiles such as the 16-electron $[\text{W}(\text{CO})_6]^{2-}$,⁹ RX, CO₂, and R₂S₂.⁹

The reaction of iron hydrides with disulfides provides synthetic access to the uncommon monomeric anionic

carbonyl thiolates.⁹ The reaction formally converts H⁻ into H⁺ concomitantly with the reduction of a disulfide to two thiolate species, a metal-bound thiolate ligand and a mercaptan (eq 1). For the poor nucleophile $\text{HFe}(\text{CO})_4^-$, the reaction was limited to PhSSPh, whereas with the more electron rich $\text{HFe}(\text{CO})_3\text{PR}_3^-$, less reactive alkyl disulfides could be used to extend the series of FeSR⁻ functionalities.¹⁰



In order to further enhance the reactivity of the hydride, we queried whether more highly substituted complexes such as $\text{HFe}(\text{CO})_2(\text{PR}_3)_2^-$ might be prepared and used in such hydride/thiolate exchange reactions. In fact, the synthesis of the bis(phosphine)-substituted hydrides by the route available to the monosubstituted hydride¹¹ (eq 2) was unsuccessful in our hands, presumably due to the diminished electrophilicity of the carbonyls in (R₃P)₂Fe(CO)₃.



The discovery of a facile, one-pot synthesis of the dihydrides $\text{H}_2\text{Fe}(\text{CO})_2(\text{P}(\text{OR})_3)_2$ (R = Ph, Et)¹² suggested an examination of deprotonation reactions as a route to the hydride anion. The report below examines this synthetic route and delineates both chemical reactivity and the structural/spectral characteristics of the unique hydride anion $\text{HFe}(\text{CO})_2(\text{P}(\text{OPh})_3)_2^-$. To our knowledge, this is the first anionic iron hydride, disubstituted with phosphorus-donor ligands, to be crystallographically characterized. Recently an analogous anion, $\text{HFe}(\text{CO})_2((\text{C}_2\text{F}_5)_2\text{PCH}_2\text{C}-\text{H}_2\text{P}(\text{C}_2\text{F}_5)_2)_2^-$, was synthesized by deprotonation of its parent dihydride.¹³

(1) Darensbourg, M. Y.; Ash, C. E. *Adv. Organomet. Chem.* 1987, 27, 1.

(2) Ellis, J. E. *Adv. Organomet. Chem.* 1990, 31, 1.

(3) Kao, S. C.; Spillet, C. T.; Ash, C. E.; Lusk, R.; Park, Y. K.; Darensbourg, M. Y. *Organometallics* 1985, 4, 83.

(4) Kristjansdottir, S.; Norton, J. R. In *Acidity of Hydrido Transition Metal Complexes in Solution. Transition Metal Hydrides: Recent Advances in Theory and Experiment*; Dedieu, A., Ed.; VCH: Deerfield Beach, FL, in press.

(5) Ash, C. E.; Delord, T.; Simmons, D.; Darensbourg, M. Y. *Organometallics* 1986, 5, 17.

(6) Ash, C. E.; Kim, C. M.; Darensbourg, M. Y.; Rheingold, A. L. *Inorg. Chem.* 1987, 26, 1357.

(7) Ash, C. E.; Darensbourg, M. Y.; Hall, M. B. *J. Am. Chem. Soc.* 1987, 109, 4173.

(8) Arndt, L. W.; Darensbourg, M. Y.; Delord, T.; Bancroft, B. T. *J. Am. Chem. Soc.* 1986, 108, 2617.

(9) Liaw, W.-F.; Kim, C.; Darensbourg, M. Y.; Rheingold, A. L. *J. Am. Chem. Soc.* 1989, 111, 3591.

(10) Darensbourg, M. Y.; Liaw, W.-F.; Riordan, C. G. *J. Am. Chem. Soc.* 1989, 111, 8051.

(11) (a) Ellis, J. E.; Chen, Y. S. *Organometallics* 1989, 8, 1350. (b) Ellis, J. E.; Chen, Y. S. *J. Am. Chem. Soc.* 1982, 104, 1141.

(12) Brunet, J.-J.; Kindela, F. B.; Labroue, D.; Neibecker, D. *Inorg. Chem.* 1990, 29, 4152.

Experimental Section

A. Methods and Materials. All reactions, sample transfers, and sample manipulations were carried out with standard Schlenk techniques (Ar atmosphere) and/or in an argon-atmosphere glovebox. All solvents were distilled under N_2 from the appropriate drying agents (hexane, tetrahydrofuran (THF), and diethyl ether from Na-benzophenone). $H_2Fe(CO)_2(P(OPh)_3)_2$ ¹² and $KBPh_4$ ¹⁴ were prepared according to literature procedures. The crown ether 18-crown-6, as well as $NaBPh_4$, $PhSSPh$, and $NaOD$ (40% weight solution in D_2O) (Aldrich), D_2O and acetone- d_6 (Cambridge Isotopes), and Et_4NOH (25% w/w in methanol) (Sigma) were used as received. THF- d_8 (Cambridge Isotopes) was stirred over Na-benzophenone and trap-to-trap vacuum-transferred. Elemental analysis was performed by Galbraith Laboratories.

B. Instrumentation. Infrared spectra were recorded on an IBM IR/32 spectrometer or a Galaxy 6021 Series FTIR instrument. NMR spectra were recorded at 200 MHz on a Varian XL-200 spectrometer.

C. Preparations and Reactions. 1. Preparation of $[Et_4N][Fe(H)(CO)_2(P(OPh)_3)_2]$. The starting material $H_2Fe(CO)_2(P(OPh)_3)_2$ (1.15 g, 1.57 mmol) was placed in a 100-mL Schlenk flask, and a 40-mL portion of THF was added to give a colorless solution. A 1.00-mL (1.71-mmol) aliquot of the methanolic $[Et_4N][OH]$ solution was added to the reaction vessel by syringe, resulting in a color change to pale yellow. The reaction mixture was stirred for 30 min, after which time the solution was concentrated to ca. 20 mL under vacuum and placed in an ice bath. Fifty milliliters of a hexane and diethyl ether mixture, in a 4:1 ratio, was layered onto the THF solution slowly, and solvent diffusion caused the formation of a pale yellow crystalline material at the solvent interface. The supernatant was removed by cannula, and the pale yellow solid was twice washed with 15 mL of degassed H_2O to remove any residual Et_4NOH . The solid was then dried under vacuum overnight; yield 1.15 g, 85%. Anal. Calcd for $C_{46}H_{51}O_9NP_2Fe$: C, 63.97; H, 5.95. Found: C, 63.79; H, 6.10. IR ($\nu(CO)$, THF): 1924 sh, 1911 m, 1838 cm^{-1} . 1H NMR (acetone- d_6): δ -10.9 (d, $J_{PH} = 57$ Hz), 6.23–6.7 (m). ^{13}C NMR (acetone- d_6): δ 224.2. ^{31}P NMR (acetone- d_6 /THF): δ 175.5 (d, $J_{PH} = 57$ Hz).

2. Preparation of $[Et_4N][(PhS)Fe(CO)_2(P(OPh)_3)_2]$. The starting material $[Et_4N][Fe(H)(CO)_2(P(OPh)_3)_2]$ (0.20 g, 0.23 mmol) was placed in a 50-mL Schlenk flask with 0.051 g (0.23 mmol) of diphenyl disulfide. A total of 25 mL of THF was added to give a yellow-orange solution. The reaction mixture was stirred for 30 min, after which time the solution was concentrated to 10 mL under vacuum. Hexane was layered in slowly, and the flask was cooled to 0 °C overnight to precipitate a golden orange semicrystalline solid. The mother liquor was removed via cannula, and the solid was washed twice with hexane. The dried orange solid weighed 0.20 g, an 88% yield. IR ($\nu(CO)$, THF): 1928 m, 1858 cm^{-1} . 1H NMR (acetone- d_6): δ 7.4–6.4 (m). ^{13}C NMR (acetone- d_6): δ 220.8. ^{31}P NMR (acetone- d_6 /THF): δ 173.4 (singlet).

D. Ion Exchange. Alkali-metal cations were replaced for Et_4N^+ cations of the $HFe(CO)_2(P(OPh)_3)_2^-$ salt using $KBPh_4$ or $NaBPh_4$ as exchange reagents. A 5-fold excess of the alkali-metal salt was typically added to a 0.06-mmol portion of the hydride in 3 mL of THF solution, resulting in the formation of a white precipitate, presumably $[Et_4N^+][BPh_4^-]$. Spectral measurements in THF were made on the supernatant without isolation of the Na^+ or K^+ salts. Five equivalents of 18-crown-6 was then added to the alkali-metal cation solution, and IR spectra were measured.

E. X-ray Crystal Structure Determination of $[Et_4N][HFe(CO)_2(P(OPh)_3)_2]$. A colorless parallelepiped (0.66 mm \times 0.80 mm \times 0.81 mm) was mounted on a glass fiber with grease, at room temperature, in a drybox and cooled to 193 K in a N_2 cold stream (Nicolet LT-2) (formula $C_{46}H_{51}NO_9P_2Fe$, formula weight 863.7). Preliminary examination and data collection were performed on a Nicolet R3m/V X-ray diffractometer (oriented graphite monochromator; Mo $K\alpha$ ($\lambda = 0.71073$ Å) radiation). Cell

Table I. Crystallographic Data for $[Et_4N][HFe(CO)_2(P(OPh)_3)_2]$

empirical formula	$C_{46}H_{51}NO_9P_2Fe$
color	colorless
habit	parallelepiped
cryst size	0.66 mm \times 0.80 mm \times 0.81 mm
space group	monoclinic, Cc (No. 9)
unit cell dimens	$a = 15.821$ (4) Å $b = 15.168$ (3) Å $c = 19.125$ (5) Å $\beta = 111.05$ (2) ^o 4283 (2) Å ³
volume	
formula units/cell	4
fw	863.7
density (calcd)	1.339 g/cm ³
abs coeff	0.476 mm ⁻¹
$F(000)$	1816 e
temp	193 K
radiation	Mo $K\alpha$ ($\lambda = 0.71073$ Å)
$R(F)$	2.33%
$R_w(F)$	3.40%

parameters (monoclinic, Cc (No. 9), $a = 15.821$ (4) Å, $b = 15.168$ (3) Å, $c = 19.125$ (5) Å, $\beta = 111.05$ (2)^o, $V = 4283$ (2) Å³, $D_{\text{exptl}} = 1.339$ g cm⁻³, $\mu = 0.476$ mm⁻¹, $Z = 4$, $F(000) = 1816$ e) were calculated from the least-squares fitting of the setting angles for 11 reflections ($2\theta_{av} = 40.7$). ω scans for several intense reflections indicated good crystal quality.

Data were collected for $5.0^\circ \leq 2\theta \leq 50.0^\circ$ (ω (Wyckoff) scans, $-17 \leq h \leq +18$, $0 \leq k \leq +18$, $-22 \leq l \leq 0$) at 193 K. Scan width, on ω , for the data collection was 0.60° , with a variable scan rate of 2.00–14.65° min⁻¹. Three control reflections, collected every 97 reflections, showed no significant trends. Background measurements by stationary crystal and stationary counter techniques were made at the beginning and end of each scan for 0.50 of the total scan time.

Systematic absences indicated that the choice of space group was either $C2/c$ or Cc . Intensity statistics favored the noncentrosymmetric space group Cc , and thus Cc was chosen for structure and refinement. Refinement of the structure in the space group $C2/c$ was attempted, but the results did not compare favorably with the results employing the choice of the space group Cc .

Lorentz and polarization corrections were applied to 4034 reflections. A semiempirical absorption correction was applied (ellipsoid approximation; $\mu_r = 0.05$; $T_{\text{max}} = 0.9497$, $T_{\text{min}} = 0.8735$). A total of 3877 unique reflections, with $|I| \geq 0.0[\sigma(I)]$, were used in further calculations. The structure was solved by direct methods (SHELXS, SHELXTL-PLUS program package).¹⁵ Full-matrix least-squares anisotropic refinement for all non-hydrogen atoms (SHELXS, SHELXTL-PLUS program package; number of least-squares parameters 523; quantity minimized $\sum w(F_o - F_c)^2$; $w^{-1} = \sigma^2 F + gF^2$, $g = 0.00090$) yielded $R = 0.023$, $R_w = 0.034$, and $S = 1.09$ at convergence (largest $\Delta/\sigma = 0.0015$; mean $\Delta/\sigma = 0.0003$; largest positive peak in the final Fourier difference map 0.49 e Å⁻³; largest negative peak in the final Fourier difference map -0.18 e Å⁻³). The Rodgers absolute configuration parameter η was refined to 0.96 (4), and the Hamilton significance test indicated the correct absolute configuration was chosen. The extinction coefficient χ (where $F^* = F_c/[1 + 0.002\chi F_c^2/(\sin 2\theta)]^{0.25}$) was refined to 0.00017 (4). The hydride ligand, H(1), was located in the Fourier difference map and its position was fixed at 1.47 Å, but it was not refined. Hydrogen atoms were placed in idealized positions with isotropic thermal parameters fixed at 0.08. Neutral atom scattering factors and anomalous scattering correction terms were taken from ref 16. A summary of the crystallographic data is in Table I. Tables giving final positional parameters and the anisotropic thermal parameters are available as supplementary material.

(15) All crystallographic calculations were performed with SHELXTL-PLUS (rev. 3.4) (G. M. Sheldrick, Institut für Anorganische Chemie der Universität, Tammannstrasse 4, D-3400 Göttingen, Federal Republic of Germany).

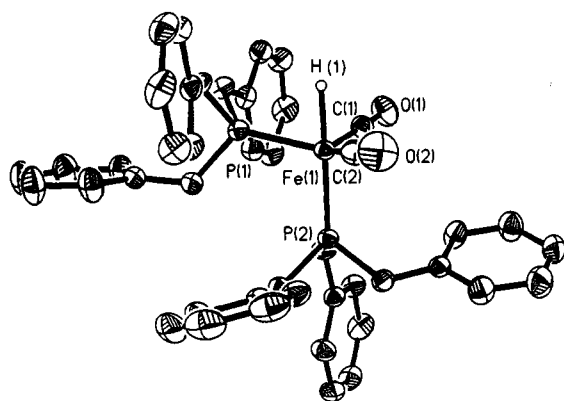
(16) *International Tables for X-ray Crystallography*; Hans, T., Ed.; D. Reidel: Dordrecht, Holland (distributed by Kluwer Academic Publishers), 1987; Vol. A, pp 101–709.

(13) Brookhart, M.; Chandler, W. A.; Pfister, A. C.; Santini, C. C.; White, P. S. *Organometallics* 1992, 11, 1263.

(14) Bhattacharyya, D. N.; Lee, C. L.; Smid, J.; Szwarc, M. *J. Phys. Chem.* 1965, 69, 608.

Table II. Selected Bond Distances and Angles for $[\text{Et}_4\text{N}][\text{HFe}(\text{CO})_2(\text{P}(\text{O}^-\text{Ph})_3)_2]$

(a) Bond Distances (Å)			
Fe-H(1)	1.469 (1)	Fe-P(2)	2.083 (1)
Fe-C(1)	1.756 (3)	C(1)-O(1)	1.154 (3)
Fe-C(2)	1.756 (2)	C(2)-O(2)	1.153 (3)
Fe-P(1)	2.076 (1)		
(b) Bond Angles (deg)			
H(1)-Fe-C(1)	85.3 (1)	C(1)-Fe-C(2)	123.1 (1)
H(1)-Fe-C(2)	80.8 (1)	P(1)-Fe-P(2)	103.2 (1)
H(1)-Fe-P(1)	76.2 (1)	C(1)-Fe-P(2)	95.6 (1)
H(1)-Fe-P(2)	179.1 (1)	C(2)-Fe-P(2)	98.9 (1)
P(1)-Fe-C(1)	109.7 (1)	Fe-C(1)-O(1)	177.9 (3)
P(1)-Fe-C(2)	119.6 (1)	Fe-C(2)-O(2)	176.7 (3)

**Figure 1.** ORTEP representation of the anion $\text{HFe}(\text{CO})_2(\text{P}(\text{O}^-\text{Ph})_3)_2^-$, showing 50% probability ellipsoids and omitting aryl hydrogens.

Results and Discussion

Synthesis. The air-stable $\text{H}_2\text{Fe}(\text{CO})_2(\text{P}(\text{O}^-\text{Ph})_3)_2$ was synthesized by the method reported by Brunet and co-workers.¹² Although the dihydride could not be deprotonated with up to 20 equiv of NEt_3 at 25 °C in THF, the anionic monohydride $[\text{Et}_4\text{N}][\text{HFe}(\text{CO})_2(\text{P}(\text{O}^-\text{Ph})_3)_2]$ was obtained on reacting a slight molar excess of $[\text{Et}_4\text{N}^+][\text{OH}^-]$ (as obtained in MeOH solution) in THF at room temperature. Upon addition of 1 equiv of HBF_4 the dihydride was re-formed (eq 3). The $[\text{Et}_4\text{N}][\text{HFe}(\text{CO})_2(\text{P}(\text{O}^-\text{Ph})_3)_2]$



salt is a pale yellow, highly air-sensitive solid which is indefinitely stable in the absence of air at room temperature. The hydride anion is highly sensitive to oxygen but is unreactive with degassed H_2O . The crystalline material is sufficiently insoluble and stable toward degassed water to permit its use as a wash to remove excess $[\text{Et}_4\text{N}^+][\text{OH}^-]$. X-ray-quality crystals were obtained from hexane/ether-THF.

Solid-State Structure of $[\text{Et}_4\text{N}][\text{HFe}(\text{CO})_2(\text{P}(\text{O}^-\text{Ph})_3)_2]$. Selected bond distances and angles for $\text{HFe}(\text{CO})_2(\text{P}(\text{O}^-\text{Ph})_3)_2^-$ may be found in Table II. A packing diagram of the salt and a complete listing of all metric data are deposited in the supplementary material. An ORTEP plot of the isolated anion (Figure 1) shows a distorted-trigonal-bipyramidal geometry in which one phosphite ligand occupies an equatorial and the other an axial position. The hydride was located in the axial position with an Fe-H distance of 1.47 Å and an $\angle\text{H-Fe-P}_{\text{ax}}$ angle of 179.1°. The greatest deviation from ideal TBP geometry lies in a bending of the CO groups and the equatorial phosphite toward the hydride site. The $\text{Fe}(\text{CO})_2\text{P}_2$ portion of the anion has considerable tetrahedral character, and

Table III. Comparison of Selected Bond Distances (Å) and Angles (deg) in Monomeric Iron Hydrides

	$[\text{HFe}(\text{C}-\text{O})_2]^{18}$	$[\text{trans-HFe}(\text{CO})_3\text{PPh}_3]^{15}$	$[\text{cis-HFe}(\text{CO})_3\text{P}(\text{O}^-\text{Ph})_3]^{16}$	$[\text{HFe}(\text{CO})_2(\text{P}(\text{O}^-\text{Ph})_3)_2]^{19}$
L_{eq}	CO	CO	$\text{P}(\text{O}^-\text{Ph})_3$	$\text{P}(\text{O}^-\text{Ph})_3$
L_{ax}	CO	PPh_3	CO	$\text{P}(\text{O}^-\text{Ph})_3$
α	98.4 (7)	99.5 (3)	95.7 (3)	103.2 (1)
β	101.9 (7)	99.5 (3)	101.3 (4)	95.6 (1)
γ	96.9 (8)	99.5 (3)	103.0 (4)	98.9 (1)
Fe-H	1.57 (12)		1.56 (7)	1.47
Fe-P _{ax}		2.187 (1)		2.083 (1)
Fe-P _{eq}			2.083 (2)	2.076 (1)
Fe-C _{ax}	1.72 (2)		1.728 (10)	
Fe-C _{eq}	1.75 (3)	1.719 (9)	1.732 (9)	1.756 (3)
C-O _{ax}	1.18 (2)		1.180 (13)	
C-O _{eq}	1.15 (3)	1.168 (8)	1.163 (8)	1.154 (3)

^a This work.

the hydride ligand may be considered as buried in the $\text{Fe}(\text{CO})_2\text{P}$ face of the tetrahedron; its stereochemical requirement forces an opening of that face.

Comparison of Solid-State Structures of Anionic Iron Hydrides. Table III compares pertinent distances and bond angles of the four known monomeric iron hydride structures, as referenced to a distorted-TBP structure. If such a description is indeed valid, the CO ligands may be viewed as equatorial in the PPh_3 derivative as well as in the bis(phosphite) anion. This position is consistent with the equatorial site preference of π -accepting ligands in a trigonal-bipyramidal geometry.¹⁷ The mono(phosphite) structure implies, however, that the site preference is not rigorously maintained for the poorer donor ligand $\text{P}(\text{O}^-\text{Ph})_3$. Between all structures the Fe-C and Fe-P bond distances do not significantly differ.

A priori, the presence of bulky P-donor ligands is expected to sterically repel the CO groups toward the hydride site. Nevertheless, the bending of the equatorial ligands toward the axial Fe-H moiety in $\text{trans-HFe}(\text{CO})_3\text{PPh}_3^-$ ($\angle\text{P}_{\text{ax}}\text{-Fe-C}_{\text{eq}} = 99.5^\circ$)⁵ is similar to that observed in $\text{HFe}(\text{CO})_4^-$, in which $\angle\text{C}_{\text{eq}}\text{-Fe-C}_{\text{ax}}(\text{av}) = 99.1^\circ$.¹⁸ $\text{cis-HFe}(\text{CO})_3(\text{P}(\text{O}^-\text{Ph})_3)^-$ permits direct comparison of $\angle\text{C}_{\text{ax}}\text{-Fe-P}_{\text{eq}}$ and $\angle\text{C}_{\text{ax}}\text{-Fe-C}_{\text{eq}}$ angles within the same ion and interestingly shows the former to be smaller.⁶ $\text{HFe}(\text{CO})_2(\text{P}(\text{O}^-\text{Ph})_3)_2^-$ displays more predictable steric effects, with the $\angle\text{P}_{\text{eq}}\text{-Fe-P}_{\text{ax}} = 103.2^\circ$ and $\angle\text{P}_{\text{ax}}\text{-Fe-C}_{\text{eq}}(\text{av}) = 97.2^\circ$.

Solution Structure of $\text{HFe}(\text{CO})_2(\text{P}(\text{O}^-\text{Ph})_3)_2^-$: Infrared and NMR Spectroscopy. The IR spectrum of the Et_4N^+ salt of $\text{HFe}(\text{CO})_2(\text{P}(\text{O}^-\text{Ph})_3)_2^-$ in CH_3CN shows two sharp bands of near-equal intensity at 1918 and 1840 cm^{-1} , assigned to the symmetric (A') and asymmetric (A'') stretches, respectively, in C_s symmetry. A very similar spectrum is obtained for THF solutions of $[\text{Na}^+][\text{HFe}(\text{CO})_2(\text{P}(\text{O}^-\text{Ph})_3)_2^-]$ to which the crown ether 18-Cr-6 has been added. The lack of base line resolution in the 1880- cm^{-1} region could be reasonably ascribed to several phenomena: impurities such as an isomeric form of the anion, a decomposition product such as $\text{Fe}(\text{CO})_3(\text{P}(\text{O}^-\text{Ph})_3)_2$, or the Fe-H stretch. The last phenomenon is consistent with observation of $\nu(\text{FeH})$ at 1895 cm^{-1} in $\text{HFe}(\text{CO})_3\text{P}(\text{O}^-\text{Ph})_3^-$.⁶

(17) (a) Rossi, A. R.; Hoffmann, R. *Inorg. Chem.* 1975, 14, 365. (b) Burdett, J. K. *Inorg. Chem.* 1976, 15, 212.

(18) Smith, M. B.; Bau, R. *J. Am. Chem. Soc.* 1973, 95, 2388.

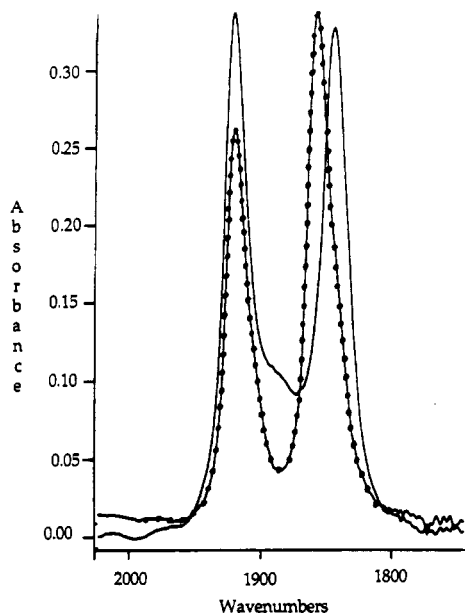
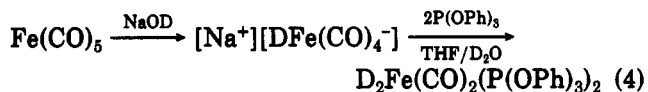


Figure 2. Overlay of $[\text{Et}_4\text{N}][\text{HFe}(\text{CO})_2(\text{P}(\text{OPh})_3)_2]$ (—) and $[\text{Et}_4\text{N}][\text{DFe}(\text{CO})_2(\text{P}(\text{OPh})_3)_2]$ (●-●) IR $\nu(\text{CO})$ spectra, at 25 °C in CH_3CN .

In pursuit of the assignment of the 1880- cm^{-1} IR feature, several attempts were made to synthesize the deuteride $\text{DFe}(\text{CO})_2(\text{P}(\text{OPh})_3)_2^-$. While hydrogen-deuterium exchange is a common reaction for many classes of terminal hydrides with d_1 alcohols or D_2O , e.g., $\text{HFe}(\text{CO})_3\text{L}^-$,¹⁹ $\text{HCr}(\text{CO})_4\text{L}^-$,²⁰ $\text{HW}(\text{CO})_4\text{L}^-$,²⁰ $\text{HRe}(\text{CO})_5$,²¹ $\text{HMn}(\text{CO})_5$,²² $\text{OsH}_2(\text{CO})(\text{PR}_3)_3$,²³ and $\text{HCo}(\text{CO})_4$,²⁴ we were unable to effect exchange of the hydride in $\text{HFe}(\text{CO})_2(\text{P}(\text{OPh})_3)_2^-$ in the presence of 10 equiv of D_2O or MeOD.

Thus, $\text{D}_2\text{Fe}(\text{CO})_2(\text{P}(\text{OPh})_3)_2$ was prepared in a manner similar to that used by Brunet et al.¹² for the synthesis of $\text{H}_2\text{Fe}(\text{CO})_2(\text{P}(\text{OPh})_3)_2$ (eq 4). The difference was that



$\text{DFe}(\text{CO})_4^-$ was generated in situ by the reaction of $\text{Fe}(\text{CO})_5$ and NaOD, and D_2O was substituted for H_2O as solvent in the subsequent reaction with 2 equiv of $\text{P}(\text{OPh})_3$. The $\text{D}_2\text{Fe}(\text{CO})_2(\text{P}(\text{OPh})_3)_2$ complex was then deprotonated with 2 equiv of $[\text{Et}_4\text{N}^+][\text{OH}^-]$ in MeOH to form $[\text{Et}_4\text{N}^+][\text{DFe}(\text{CO})_2(\text{P}(\text{OPh})_3)_2^-]$. (Since the H/D exchange reactions were negative for H_2O or MeOH, it was not necessary to use $[\text{Et}_4\text{N}^+][\text{OD}^-]$ in MeOD.) The CH_3CN solution $\nu(\text{CO})$ IR spectrum of $[\text{Et}_4\text{N}^+][\text{DFe}(\text{CO})_2(\text{P}(\text{OPh})_3)_2^-]$ showed clear base line resolution between the two bands at 1918 and 1854 cm^{-1} . Overlays of the CH_3CN solution spectra of $\text{HFe}(\text{CO})_2(\text{P}(\text{OPh})_3)_2^-$ and $\text{DFe}(\text{CO})_2(\text{P}(\text{OPh})_3)_2^-$ as Et_4N^+ salts are shown in Figure 2. Both the shift in the lower frequency $\nu(\text{CO})$ band²⁵ and the base line resolution between the two bands on replacing H with D are consistent with assignment of the 1880- cm^{-1} feature to the Fe-H stretch. On the basis of this assignment, the Fe-D

Table IV. ^1H NMR (ppm) and $\nu(\text{CO})$ Band Positions (cm^{-1}) for Solutions^a of $[\text{cation}^+][\text{HFe}(\text{CO})_2(\text{P}(\text{OPh})_3)_2^-]$

cation ⁺	$\nu(\text{CO})$	^1H NMR (THF- d_6 , acetone- d_6)
Et_4N	1919 (s), 1840 (s) ^b	
Et_4N	1928 (sh), 1911 (s), 1833 (vs)	-10.9 (t, $J_{\text{PH}} = 57$ Hz)
Na	1916 (s), 1820 (vs)	-10.8 (t, $J_{\text{PH}} = 54$ Hz)
Na + Cr ^c	1919 (s), 1841 (s)	
K	1914 (s), 1826 (vs)	-10.9 (t, $J_{\text{PH}} = 49$ Hz)
K + Cr ^c	1922 (s), 1844 (s)	

^a THF solution spectra except where noted. ^b CH_3CN solution. ^c 18-crown-6.

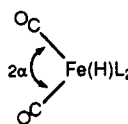
stretch is calculated to be at 1320 cm^{-1} ; however, due to overlapping bands in that region, no definite identification could be made.

The resolution of the $\nu(\text{CO})$ region in the $[\text{Et}_4\text{N}^+][\text{DFe}(\text{CO})_2(\text{P}(\text{OPh})_3)_2^-]$ solution IR spectra permitted measurement of $\nu(\text{CO})$ IR intensity ratios in the absence of Fe-H coupling. These were applied toward the calculation of the internal CO-Fe-CO angle in accordance with a procedure described by Darensbourg.²⁶ Equations 5 and 6 were used to calculate the internal angle, where $I_1^{(A)}$ and

$$I_1^{(A)} = 2G_{\text{tt}}[\cos^2 \alpha(\mu'_{\text{MCO}})^{(1)2}] \quad (5)$$

$$I_1^{(A')} = 2G_{\text{tt}}[\sin^2 \alpha(\mu'_{\text{MCO}})^{(2)2}] \quad (6)$$

$I_2^{(A')}$ are the measured intensities ($\times 10^{-4}$) of the bands at 1918 and 1854 cm^{-1} , respectively. G_{tt} is the inverse mass of a CO group (0.14585); $\mu'_{\text{MCO}}^{(1)}$ and $\mu'_{\text{MCO}}^{(2)}$ are the group dipole moment changes with respect to the CO stretch in each MCO group in the symmetric and antisymmetric stretch; α is half the angle between the MCO groups:



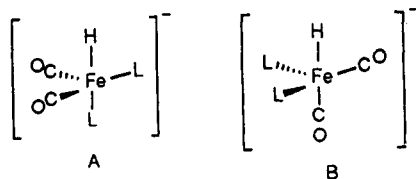
The measured peak areas of the symmetric and asymmetric CO stretches gave an $I(A)/I(A')$ ratio of 0.67. Assuming that $\mu'_{\text{MCO}}^{(1)}$ and $\mu'_{\text{MCO}}^{(2)}$ are equal,²⁶ α was calculated to be 50.7°, and thus the CO-Fe-CO angle equals 101.4°. Therefore, the angle calculated from the solution spectral data is clearly much less than that obtained in the X-ray solid-state structure of $\text{HFe}(\text{CO})_2(\text{P}(\text{OPh})_3)_2^-$ (123.1°). However, the 101.4° angle is very similar to the axial/equatorial $\angle\text{OC-Fe-CO}$ seen in $\text{HFe}(\text{CO})_3\text{P}(\text{OPh})_3^-$, in which the phosphite ligand is in an equatorial position.⁶ It is also consistent with $\angle\text{CO}_{\text{ax}}\text{-Fe-CO}_{\text{eq}} = 99.1^\circ$ in $\text{HFe}(\text{CO})_4^-$ and $\angle\text{PPh}_3\text{-ax-Fe-CO}_{\text{eq}} = 102.2^\circ$ in $\text{HFe}(\text{CO})_3\text{PPh}_3^-$.^{5,18} This result indicates that the solution-state structure of $\text{DFe}(\text{CO})_2(\text{P}(\text{OPh})_3)_2^-$ and thus the analogous hydride differs from the solid-state structure of $\text{HFe}(\text{CO})_2(\text{P}(\text{OPh})_3)_2^-$.

The proton NMR spectra of $\text{HFe}(\text{CO})_2(\text{P}(\text{OPh})_3)_2^-$ salts corroborate the structural implications of the IR results. As shown in Table IV, a triplet centered at -10.9 ppm is observed in THF or acetone solutions of the hydride anion, with phosphorus-hydrogen scalar coupling constants ranging from 49 to 57 Hz, dependent on the counterion. These J_{PH} values are independent of temperature (from -80 to +25 °C). Had the solid-state structure been maintained in solution in static form, a doublet of doublets would be predicted, on the basis of the fact that *trans*- $\text{HFe}(\text{CO})_3\text{PR}_3^-$ (R = OMe, Ph) showed J_{PH} coupling constants distinctly different from those of *cis*- $\text{HFe}(\text{CO})_3\text{P}$ -

(19) Ash, C. E. Ph.D. Dissertation, Texas A&M University, 1987.
 (20) Gaus, P. L.; Kao, S. C.; Darensbourg, M. Y.; Arndt, L. W. *J. Am. Chem. Soc.* 1984, 106, 4752.
 (21) (a) Beck, W.; Hieber, W.; Braun, G. Z. *Anorg. Allg. Chem.* 1961, 308, 23. (b) Braterman, P. S.; Harril, R. W.; Kaesz, H. D. *J. Am. Chem. Soc.* 1967, 89, 2851.
 (22) Andrews, M. A.; Kirtley, S. W.; Kaetz, H. D. *Adv. Chem. Ser.* 1978, No. 167, 215.
 (23) Vaska, L. *J. Am. Chem. Soc.* 1966, 88, 4100.
 (24) Ungvary, F.; Marko, L. *Organometallics* 1983, 2, 1608.
 (25) Walker, H. W.; Ford, P. C. *Inorg. Chem.* 1982, 21, 2509.

(26) Darensbourg, D. J. *Inorg. Chem.* 1972, 11, 1606.

$(\text{OPh})_3^-$ (vide supra). If a rapid equilibration of isomeric forms A and B averaged the coupling constants, one might



expect J_{PH} values no higher than 30–40 Hz (based on a maximum of 12 Hz for the trans J_{PH} value and 60 Hz for cis J_{PH}) and a dependence on temperature.^{5,6} A ground-state structure in which both P-donor ligands are in equatorial sites, i.e., structure B, is thus most consistent with the ^1H NMR spectrum and is also consistent with the observed doublet ($J_{\text{PH}} = 57$ Hz) in the ^{31}P NMR spectrum. Certainly the anion is fluxional, as evidenced by the observation of a singlet at δ 224.2 in the ^{13}C NMR spectrum. This rapid exchange of the carbonyl ligands is also observed in the ^{13}C NMR spectrum of *cis*- $\text{HFe}(\text{CO})_2\text{P}(\text{OPh})_3^-$, which contains a singlet at δ 224 at temperatures as low as -110°C .⁶

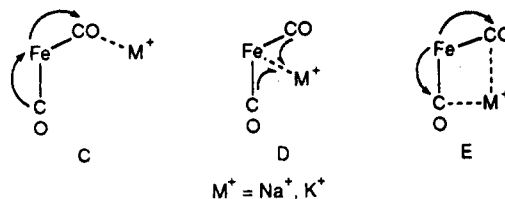
Another interpretation of the two isomeric forms A and B is that formal addition of a hydride ligand along the $\text{L}_2\text{Fe}(\text{CO})_2$ pseudotetrahedron easily generates B, the geometrical form seen in solution; addition along the $\text{L}(\text{CO})_2$ face generates form A, the geometry in the solid state.

Note that the intensity ratio of the A' to A'' bands is a simple inverse tangent function of $\angle\text{OC-Fe-CO}$; a single band would result from a 180° angle, and two bands of equal intensity would result from a 90° angle between the CO groups. Thus, in the absence of significant M-H coupling, an approximate structure can be deduced from inspection of the $\nu(\text{CO})$ IR pattern.

Ion Pairing. The interactions of cations with anionic hydrido carbonylates have been used to indicate the site of greatest electron density in the anions.^{1,5} Experimentally this is accomplished by comparison of the $\nu(\text{CO})$ IR spectra of solutions containing the anion in a form unperturbed by interacting cations with spectra measured on salts dissolved in solvents of low dielectric constant which would promote contact ion pairing. The $\nu(\text{CO})$ IR spectrum of the $\text{HFe}(\text{CO})_2(\text{P}(\text{OPh})_3)_2^-$ anion, unperturbed by interacting cations, is taken to be that of the Et_4N^+ salt in CH_3CN solution, which was presented above, or that of THF solutions of the alkali-metal-cation salts to which a crown ether has been added. Earlier work has shown that the conductivity of such solutions is relatively small, and the ions are mainly present as solvent-separated ion pairs, *ssip*'s.²⁷

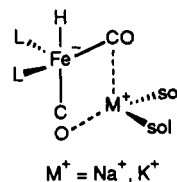
Table IV contains the $\nu(\text{CO})$ IR spectral data for the Et_4N^+ , Na^+ , and K^+ salts of $\text{HFe}(\text{CO})_2(\text{P}(\text{OPh})_3)_2^-$ in THF and in CH_3CN solutions. In THF solution, Et_4N^+ is found to perturb the $\nu(\text{CO})$ IR spectrum of $\text{HFe}(\text{CO})_2(\text{P}(\text{OPh})_3)_2^-$ as compared to the CH_3CN solution spectrum described above. The effect is a shifting of both bands by -7 or -8 cm^{-1} . In addition, a shoulder developed at 1928 cm^{-1} on the higher frequency band. Such complexities have previously been observed in solution spectra of other carbonylate anions as their Et_4N^+ salts and are presumed to be due to delocalized, but ill-defined, ion-pair interactions and ion-pair equilibria.^{28,29}

The IR spectra of the Na^+ and K^+ salts of $\text{HFe}(\text{CO})_2(\text{P}(\text{OPh})_3)_2^-$ in THF showed a shift of both CO absorptions to lower frequencies as compared to the solutions to which the 18-crown-6 alkali-metal-ion sequestering agent had been added. The higher frequency band is shifted least, by only 3 cm^{-1} , while the lower is shifted by ca. 20 cm^{-1} (Table IV). The fact that both bands shift to lower frequencies is in contrast to the usual examples of site-specific alkali-metal-cation interactions with carbonylates.²⁸ Most commonly, alkali-metal-cation interaction with one CO group (structure C) lowers the CO stretching frequency



as electron density is polarized onto it via π -back-bonding, concomitant with a reduction of π -back-bonding to those CO groups that do not encounter a contact ion pair interaction and an increase in their $\nu(\text{CO})$ values.²⁸ In comparable cases, such as the $\text{H}(\text{MeO})_3\text{PFe}(\text{CO})_2\text{CO}\cdots\text{Na}^+$ interaction,⁵ the lowering of $\nu(\text{CO})$ values for the $\text{Fe-CO}\cdots\text{Na}^+$ contact is larger ($\Delta\nu(\text{CO}) \approx 30$ cm^{-1}) than that observed here ($\Delta\nu(\text{CO}) \approx 20$ cm^{-1}). Had the Na^+ interaction withdrawn electron density from the Fe (structure D) or H site without interaction with CO groups, both $\nu(\text{CO})$ absorptions would have experienced an increase in value due to reduced π -back-bonding.

Hence, the evidence suggests that the Na^+ simultaneously interacts with two CO groups, as indicated in structure E and by



Such an intimate ion pair is reminiscent of the solid-state structure of alkali-metal salts of $\text{Fe}(\text{CO})_4^{2-}$ which indicate similar cation interactions with the OC-Fe-CO " π -allylic pocket".³⁰ The extent to which the cation engages the electron density localized on iron is definitely greater in the dianion. The contact ion pair structure we propose maintains an axial/equatorial position of CO groups consistent with the similarity in intensity patterns in the IR spectrum of the alkali-metal contact ion pairs with that of the *ssip*.

Chemical Reactivity. Upon addition of PhSSPh to a pale yellow solution of $[\text{Et}_4\text{N}][\text{HFe}(\text{CO})_2(\text{P}(\text{OPh})_3)_2]$ in THF at room temperature, an immediate reaction occurred to form an orange solution. The isolated orange solid was redissolved in acetone- d_6 , and NMR spectra were characterized by multiplets in the 7.6–6.4 ppm range (^1H NMR), the lack of a resonance in the high-field iron-hydride region, and a singlet in the ^{31}P NMR spectrum. The $\nu(\text{CO})$ signal in THF showed a two-band pattern at 1928 (m) and 1858 (s) cm^{-1} , which are shifted to slightly higher energies as compared to the parent hydride anion and are similar to what was earlier noted for hydride/thiolate exchange reactions in iron carbonylates.^{5,6} The

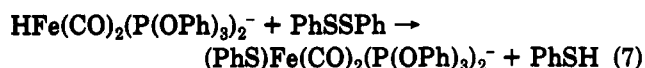
(27) Darenbourg, M. Y.; Barros, H. L.; Borman, C. *J. Am. Chem. Soc.* 1977, 99, 1647.

(28) Darenbourg, M. Y. *Prog. Inorg. Chem.* 1985, 33, 221.

(29) Darenbourg, M. Y.; Sackett, J. R.; Jiminez, P.; Hanckel, J. M.; Kump, R. L. *J. Am. Chem. Soc.* 1982, 104, 1521.

(30) (a) Teller, R. G.; Finke, R. G.; Collman, J. P.; Chin, H. B.; Bau, R. *J. Am. Chem. Soc.* 1977, 99, 1104. (b) Bau, R. *J. Am. Chem. Soc.* 1976, 98, 2434.

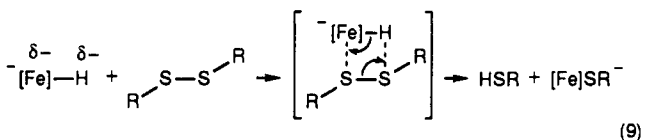
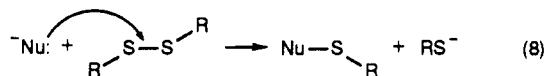
new compound is presumed to be $[\text{Et}_4\text{N}][(\text{PhS})\text{Fe}(\text{CO})_2(\text{P}(\text{OPh})_3)_2]$ (eq 7). The intensity ratio of the two $\nu(\text{CO})$



IR bands, ca. 0.29, predicts an $\angle\text{OC-Fe-CO}$ angle of ca. 123° , consistent with a TBP structure in which the benzenethiolate ligand is in an axial position and the carbonyl ligands are each in equatorial positions. This is in contrast with the proposed solution-state configuration of $\text{HFe}(\text{CO})_2(\text{P}(\text{OPh})_3)_2^-$ (vide supra). The anionic thiolate is stable in solution under argon overnight, but decomposition is evident even at -20°C in the solid state over a period of 1 week, hampering elemental analysis.

Attempts to extend the hydride/thiolate redox-based exchange reaction to alkyl disulfides, Me_2S_2 and $t\text{-Bu}_2\text{S}_2$, were unsuccessful. On the basis of the observed reactivity of the $\text{HFe}(\text{CO})_3\text{PR}_3^-$ anions with the dialkyl disulfides as well as the diaryl disulfides, the lack of reactivity of with Me_2S_2 was of concern.

Both single-electron-transfer pathways and a nucleophilic replacement reaction³¹ (eq 8) are possible mechanisms for disulfide cleavage reactions with anionic hydrides. The collision complex expected for the latter path



and visualized in eq 9 draws on calculations of charge distribution in the $\text{HFe}(\text{CO})_4\text{L}_x^-$ anions which assign a large negative character to the Fe center.¹⁰ Certainly such an encounter would experience more steric hindrance in the bis(phosphite) hydride as compared to the $\text{HFe}(\text{CO})_3\text{PR}_3^-$ complexes. However, those steric hindrances are not prohibitive to the formation of the $(\text{PhS})\text{Fe}(\text{CO})_2(\text{P}(\text{OPh})_3)_2^-$ anion and should not be restrictive for the SMe^- derivative. In the absence of kinetic data to establish the molecularity of the hydride/thiolate exchange reaction, further mechanistic speculation is unwarranted.

There are thermodynamic as well as kinetic factors to be considered in delineating the H^-/SR^- exchange reaction, including (1) the Fe-H bond strength, which is expected to increase as the number of P-donor ligands increase, and (2) the destabilization of Fe-S-alkyl as compared to Fe-S-aryl interactions due to the antibonding character of sulfur lone pair interactions with filled d_{xz} and d_{yz} orbitals on iron.^{32,33} In the case of the $\text{HFe}(\text{CO})_2(\text{P}(\text{OPh})_3)_2^-$ anion

both factors oppose our goal of preparing a series of $(\text{RS})\text{Fe}(\text{CO})_2(\text{P}(\text{OPh})_3)_2^-$ anions. Nevertheless, alternative routes to the thiolate anions must be explored prior to definitive conclusions regarding stability.

Concluding Comments. The above solid-state/solution-state isomerism of the $\text{HFe}(\text{CO})_2(\text{P}(\text{OPh})_3)_2^-$ anion illustrates the balance of steric/electronic effects that make geometrical site preferences in multiligated TBP structures less than predictable by theory. That is, the conclusions drawn from overlap and symmetry arguments for penta-coordinate complexes, presented by Rossi and Hoffmann with prudent notes as to their limitations^{17a} and by Burdett with similar caution regarding possible oversimplicity,^{17b} must be viewed as first approximations only when applied to distorted, multiligated complexes such as the one described above. Appropriate to our problem are the axial/equatorial isomerisms observed in the $\text{LM}(\text{CO})_4$ ($\text{M} = \text{Fe}, \text{Ru}, \text{Os}$; $\text{L} = \text{ER}_3$ ($\text{E} = \text{P}, \text{Sb}, \text{As}$)) series of TBP complexes.³⁴ Einstein, Pomeroy, and Martin concluded that arguments based on the σ -accepting, π -back-bonding ability of the metal can indeed rationalize the observed order with respect to the tendency to generate the equatorial isomer: $\text{Ru} > \text{Os} \gg \text{Fe}$ and $\text{Sb} > \text{As} > \text{P}$.³⁴ We suggest that the anionic hydride ligand imparts to iron better π -back-bonding capabilities (perhaps rivaling that of Ru?) and poorer σ -acceptor ability and enhances the potential for $\text{P}(\text{OPh})_3$ occupancy of the equatorial site. Such an axial/equatorial potential must be so poised that crystal-packing forces and solvent interactions are sufficient to enable isomeric "switchovers".³⁴

Acknowledgment. This work was supported by the National Science Foundation (Grant No. CHE-9109579). Funding for the X-ray diffractometer and crystallographic computing system (Grant No. CHE-8513273) was also provided by the National Science Foundation. We wish to thank Prof. D. J. Darensbourg for enlightening discussion and Robert Espina for his technical assistance.

Note added in proof: After this paper was submitted, the syntheses of the salts $[\text{K}^+][\text{HFe}(\text{CO})_2(\text{PR}_3)_2^-]$ ($\text{R}_3 = n\text{-Bu}_3, \text{Me}_2\text{Ph}$) were reported by Brunet et al., along with solution-state spectral properties.³⁵

Supplementary Material Available: Tables of atom positional parameters, bond lengths, bond angles, and anisotropic displacement parameters and a packing diagram and a fully labeled ORTEP representation of $[\text{Et}_4\text{N}][\text{HFe}(\text{CO})_2(\text{P}(\text{OPh})_3)_2]$ (8 pages). Ordering information is given on any current masthead page.

(32) Darensbourg, M. Y.; Longridge, E. L.; Payne, V. A.; Reibenspies, J. H.; Riordan, C. G.; Springs, J. J.; Calabrese, J. C. *Inorg. Chem.* **1990**, *29*, 2721.

(33) Ashby, M. T. *Comments Inorg. Chem.* **1990**, *10*, 297.

(34) Martin, L. R.; Einstein, F. W. B.; Pomeroy, R. K. *Inorg. Chem.* **1985**, *24*, 2777.

(35) Brunet, J.-J.; Commenges, G.; Kindela, F.-B.; Neibecker, D. *Organometallics* **1992**, *11*, 1343.

(31) Kice, J. L.; Favstritaky, N. A. *J. Am. Chem. Soc.* **1969**, *91*, 1751.